Three-Particle Final State Energy Distributions: T+D $\rightarrow n+\alpha+\gamma$ and T+T $\rightarrow 2n+\alpha$

Carl R. Brune

Ohio University

3 December 2013

Los Alamos National Laboratory – Seminar

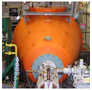

T$(d,\gamma)^5$He* and T$(t,2n)\alpha$

- Both play an important role in inertial confinement fusion:
  - T$(d,\gamma)^5$He*: γ rays $\rightarrow$ GRH
  - T$(t,2n)\alpha$: neutron $\rightarrow$ NTOF, MRS
- Both involve the unbound ^{5}He nucleus
- $\alpha + n$ (^{5}He) resonances effect the energy distributions
- R-Matrix description of 3-particle final states?
- Both final-state energy spectra are not "well known" experimentally

^{5}He Level Properties are Well Know from ^{4}He(n, n) Studies

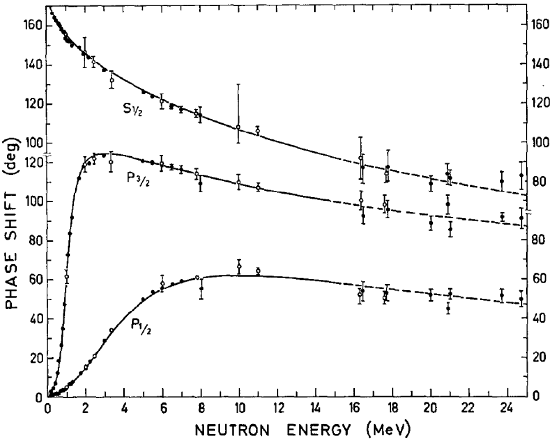

Stammbach and Walter (1972)

Determinations of the widths of these states may differ...

Nuclear Physics **A366** (1981) 299–319

REACTION DEPENDENCE OF NUCLEAR DECAY LINEWIDTHS

D. OVERWAY and J. JÄNECKE [†]
Department of Physics, University of Michigan, Ann Arbor, Michigan 48109, USA

F. D. BECCHETTI
Department of Physics, University of Michigan, Ann Arbor, Michigan 48109, USA
and
Hahn-Meitner Institute [††], Berlin 39, W. Germany

C. E. THORN
Department of Physics, Brookhaven National Laboratory [‡], Upton, LI, NY, 11973, USA

and

G. KEKELIS
Department of Physics and Astronomy, Williams College, Williamstown, Mass. 01267, USA

- Energy dependence of penetrability factors
- 3-body final-state interactions
- Coherent interference with other processes of the same J^π
- Background from processes with possibly different J^π
- $\rightarrow$ Observed linewidth may vary with reaction and kinematics
- Well-studied for the first 2^+ state in ^{8}Be

Edwards Accelerator Laboratory

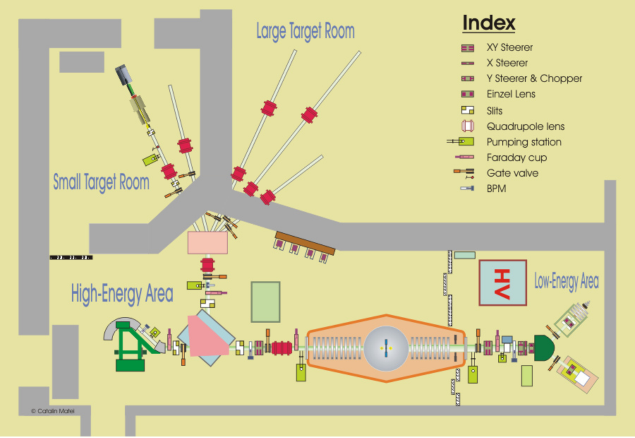

- 4.5-MV Tandem Accelerator
- Pelletron Upgrade in 2011/12 via $321k NSF MRI grant
- Unique beam swinger and 30-m TOF tunnel
- Specializations: TOF techniques, neutrons
- `http://inpp.ohiou.edu/~oual/`

^{3}H(d,γ) Branching Ratio and Photon Spectrum

Used as a γ-ray diagnostic for the National Ignition Facility. Both the branching ratio relative to ^{3}H(d,n) and the γ-ray spectrum are important.

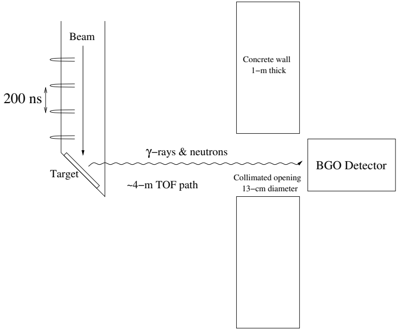

A pulsed 500-keV deuteron beam was used in conjunction with a stopping-thickness solid ^{3}H target at the Edwards Accelerator Laboratory. A 4"×4" BGO detector placed in the beam swinger tunnel ≈ 4 m from the target. Key personnel: Cody Parker, Tom Massey, Carl Brune.

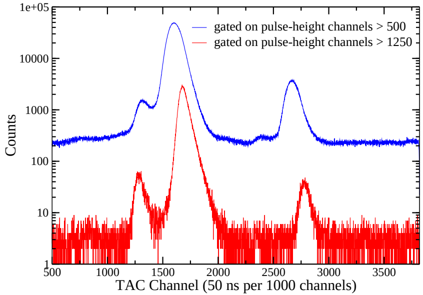

Time-of-flight spectra for two pulse-height gates.

^{3}H(d,γ) Results and Future Plans

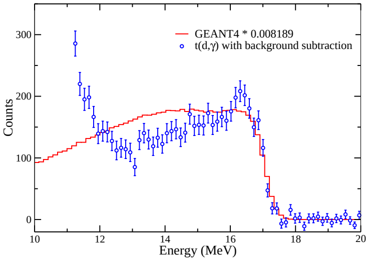

Background-subtracted γ-ray spectrum and Monte Carlo prediction for shape.

- $\langle E_{c.m.} \rangle = 196$ keV
- $R = (6.9 \pm 1.6) \times 10^{-5}$
- Several improvements are underway:
  - new low-mass target holder
  - fresh tritium target
  - α-particle monitor
- Talk to Cody Parker for more details
- Theoretical work planned at TRIUMF (P. Navratil)

Comparison to Previous Work

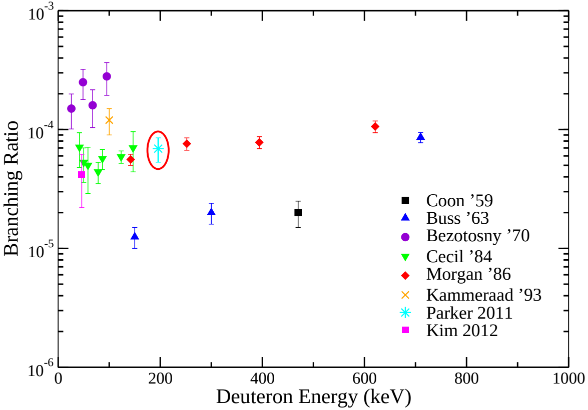

R-Matrix Model for ^{3}H(d,γ)

- In general, the full suite of partial waves in the initial and final state and γ-ray multipolarities would need to be considered:

$$\frac{d\sigma}{dE_\gamma} \propto |\langle d+t|H_{EM}|n+\alpha\rangle|^2$$

- Limiting ourselves to $3/2^+$ in the initial state and considering $E1$ transitions to the $1/2^-$ and $3/2^-$ final states is reasonable
- Use R-matrix formulas (following Barker):

$$\frac{d\sigma}{dE_\gamma} = E_\gamma^3 P_l \left| \frac{\sum_\lambda \frac{A_\lambda \gamma_\lambda}{E_\lambda - E}}{1-(S_l - B + iP_l)R} \right|^2 \qquad R = \sum_\lambda \frac{\gamma_\lambda^2}{E_\lambda - E}$$

- Includes penetrabilities and coherent interference
- E_λ and γ_λ are determined from $n-\alpha$ elastic scattering
- A_λ are γ-ray feeding factors
- Only 2 levels are needed for both final states

R-Matrix Results for $^3H(d, \gamma)$

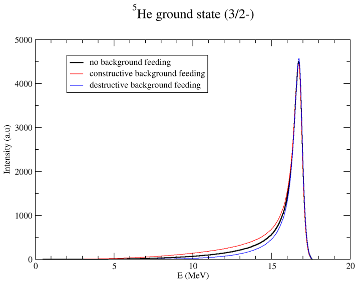

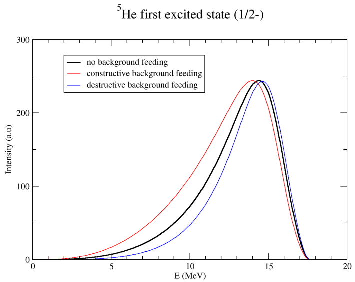

- Colored curves show possible effects of coherent interference (maximum plausible)
- Similar to “Hale Spectrum”
- Except the present $3/2^-$ width is 0.70 MeV – versus 0.50 MeV and there is more strength in the tail of the $3/2^-$ peak

Hale Spectrum: “Two-Body Resonance Model”

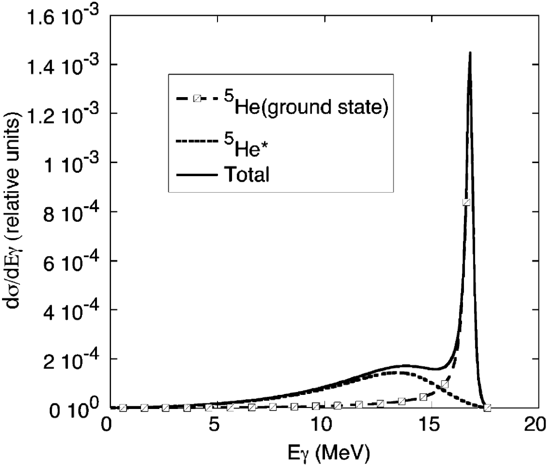

J.M. Mack, G.M. Hale et al., Rad. Phys. and Chem. **75** 551-556 (2006).

$T(t, 2n)\alpha$

- Wong, Anderson et al. results (1965)
- R-matrix model
- National Ignition Facility results
- Role of di-neutron emission?
- How to resolve ambiguities?
- α spectrum?
- $T(t, 2n)$ absolute cross section?
- $^3\mathrm{He}(^3\mathrm{He}, 2p)\alpha$ and $^3\mathrm{He}(t, np)\alpha$

$T(t, 2n)\alpha$ Neutron Spectrum
$E_{c.m.} = 200$ keV

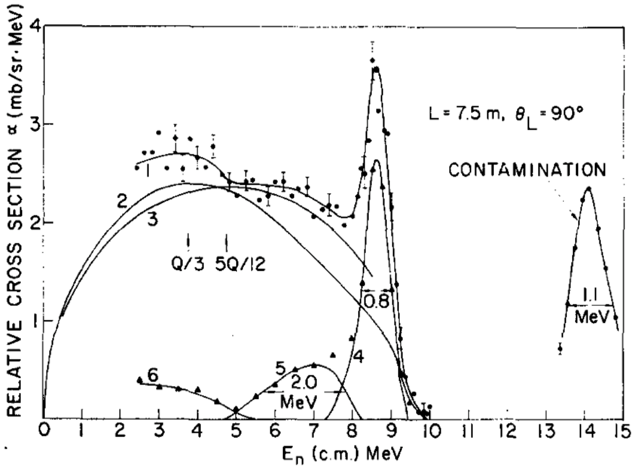

Wong, Anderson, and McClure (1965)

$T(t, 2n)\alpha$ R-Matrix Modeling

Carl Brune, Dan Sayre, Jac Caggiano, Gerry Hale, Mark Paris

- Sequential decay model
- Kinematics (recoil) is more complicated
- Angular correlation effects on spectrum
- Identical particles / antisymmetrization
- F.C. Barker formalism + angular momentum coupling + antisymmetrization
  - D.P. Balamuth, R.W. Zurmühle, and S.L. Tabor, Phys. Rev. C **10**, 975 (1974).
  - D.F. Geesaman *et al.*, Phys. Rev. C **15**, 1835 (1977).
  - H.O.U. Fynbo *et al.*, Phys. Rev. Lett **91**, 082502 (2003).

Some Formulas

- Our form for the matrix element:

$$\mathcal{M}_{\nu_1\nu_2} = \sum_c u_c(12) f^{lJ}_{\nu_1\nu_2}(\Omega_1, \Omega_{23}) - u_c(21) f^{lJ}_{\nu_2\nu_1}(\Omega_2, \Omega_{13})$$

- u_c is given by an R-matrix expression:

$$u_c(12) = \left[\frac{P_1 P_{23}}{p_1 p_{23}}\right]^{1/2} e^{i(\omega_1 - \Phi_1)} e^{i(\omega_{23} - \Phi_{23})} \frac{\sum_\lambda \frac{A_{c\lambda}\gamma_{c\lambda}}{E_{c\lambda} - E_{23}}}{1 - [S_{23} - B_c + iP_{23}]R_c}$$

- $f^{lJ}_{\nu_1\nu_2}$ contains the spin and angular information:

$$f^{lJ}_{\nu_1\nu_2}(\Omega_1, \Omega_{23}) = \sum_{m, m_l, m_l'} \frac{(-1)^{J+m}}{\sqrt{2J+1}} \langle l m_l \tfrac{1}{2} \nu_1 | J m \rangle \langle l m_l' \tfrac{1}{2} \nu_2 | J {-m} \rangle Y_{l m_l}(\hat{\boldsymbol{p}}_1) Y_{l m_l'}(\hat{\boldsymbol{p}}_{23})$$

- The particle distribution is given by

$$\frac{d^3 N}{dE_i\, \Omega_i\, d\Omega_j} = \sum_{\nu_1, \nu_2} |\mathcal{M}_{\nu_1\nu_2}|^2 \, p_i p_{jk} \mathcal{J}_{ijk}$$

- A 0^+ ($l = 0$) initial $t + t$ state is assumed, and $c = 1/2^+$, $1/2^-$, $3/2-$ $n + \alpha$ or an $l = 0$ spin-singlet dineutron state.

The resulting formula for the particle spectra...

is not so simple, and I will not repeat it here. The key step is the application of an obscure addition theorem for spherical harmonics that was first given by M.E. Rose [Journal of Mathematics and Physics **37**, 215 (1958)]:

$$Y_{lm}(\hat{\boldsymbol{c}}) = \sum_{\substack{\lambda_1+\lambda_2=l \\ \nu_1+\nu_2=m}} a^{\lambda_1} b^{\lambda_2} \langle \lambda_1 \nu_1 \lambda_2 \nu_2 | lm \rangle \sqrt{\frac{4\pi(2l+1)!}{(2\lambda_1+1)!(2\lambda_2+1)!}} Y_{\lambda_1 \nu_1}(\hat{\boldsymbol{a}}) Y_{\lambda_2 \nu_2}(\hat{\boldsymbol{b}}),$$

where $\hat{\boldsymbol{c}} = \vec{\boldsymbol{a}} + \vec{\boldsymbol{b}}$ with $\vec{\boldsymbol{a}} = a\hat{\boldsymbol{a}}$ and $\vec{\boldsymbol{b}} = b\hat{\boldsymbol{b}}$.

Findings:

- Antisymmetrization is very important
- Angular correlations are important for the $3/2^-$ $n+\alpha$ channel
- There *is* coherent interference between different partial waves

Neutron Energy Distributions

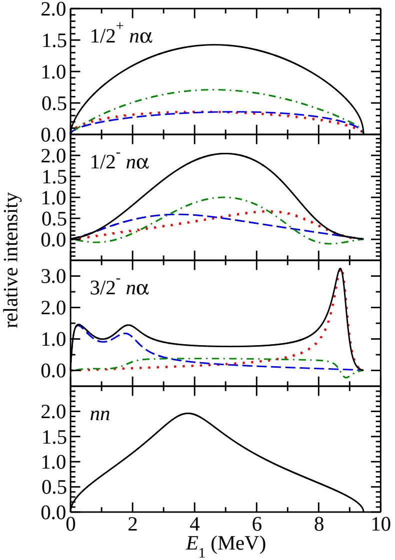

Neutron energy distributions for each channel considered separately. The primary, secondary, exchange, and total are given by the dotted, dashed, dot-dashed, and solid curves, respectively. Only the total is shown for the nn case.

Coherent Interference Effects

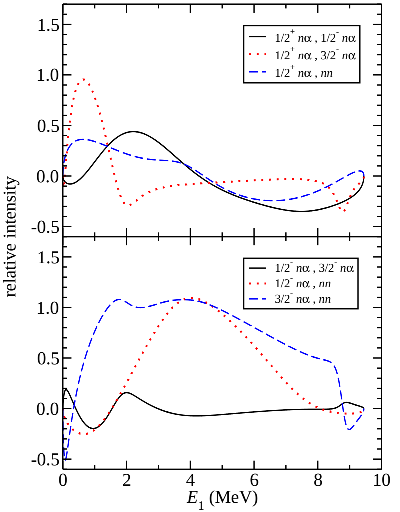

- Interference contributions to the neutron energy distributions for partial wave combinations indicated.
- There is minimal coherent interference between the 3/2− and 1/2− contributions.

Measurement of the $T(t, 2n)\alpha$ Neutron Spectrum at the National Ignition Facility

- Nearly pure tritium gas (0.1% D), low areal density "symcap"
- $kT = 3.3(3)$ keV $\quad\rightarrow\quad E_{\text{Gamow}}(\text{T} + \text{T}) = 16$ keV
- 2 organic liquid scintillators (xylene) @ 20 and 22 meters, respectively
- Modeling includes:
  - Instrument Response Function (time response)
  - Scintillator response (efficiency)
  - Attenuation and scattering
  - Thermal broadening
  - Background from T(d, n) (small)
- Dan Sayre, Jac Caggiano, Robert Hatarik, Chris Hagmann, Tom Phillips, and many additional collaborators (including CRB and ADB).

Raw Data from Equator Detector @ 20.1 m

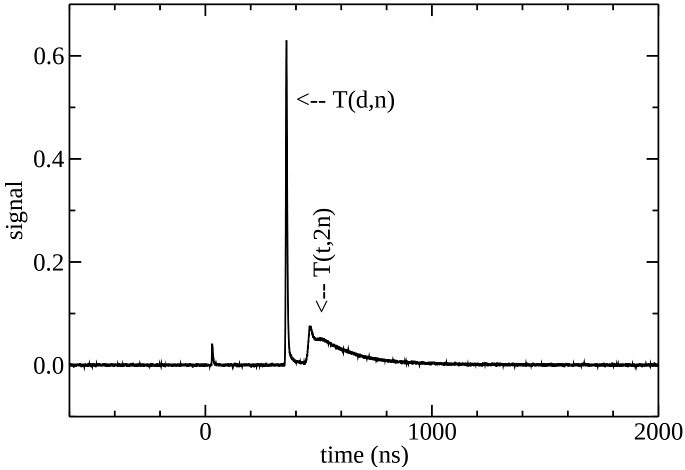

R-Matrix Fit

- Assume $3/2^-$ and $1/2^-$ n-α channels.
- Use the Stammbach and Walter n-α R-matrix parameters
- Fit both detectors simultaneously
- Achieve $\chi^2_\nu = 2.2$ (statistical errors are complicated)
- Results:

J^π	λ	E_λ (MeV)	γ^2_λ (MeV)	A_λ
$3/2^-$	1	0.97	7.55	11.1
$3/2^-$	2	100.0	30.0	157
$1/2^-$	1	6.43	12.3	19.6
$1/2^-$	2	100.0	30.0	689

Fits to Time Spectra

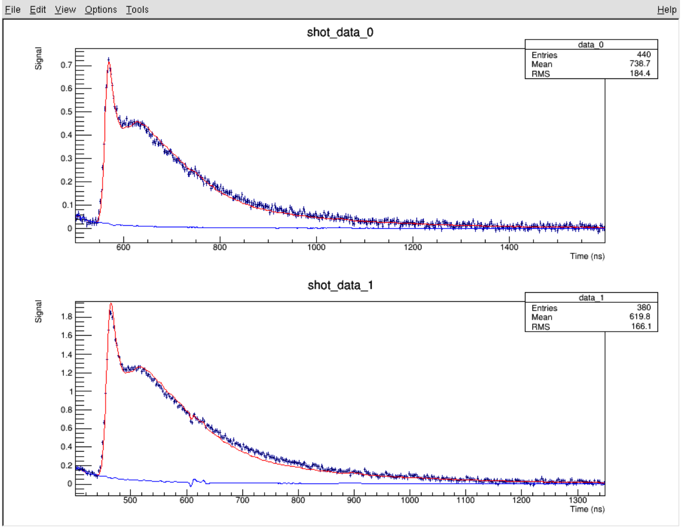

$T(t, 2n)\alpha$ Neutron Spectrum
$E_{c.m.} = 16$ keV

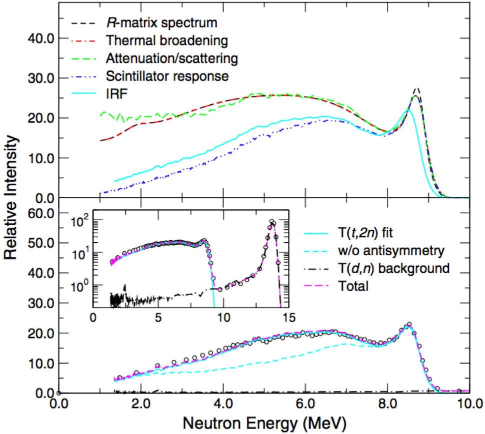

Sayre, Caggiano et al. (2013) @ NIF

α Particle Energy Distributions

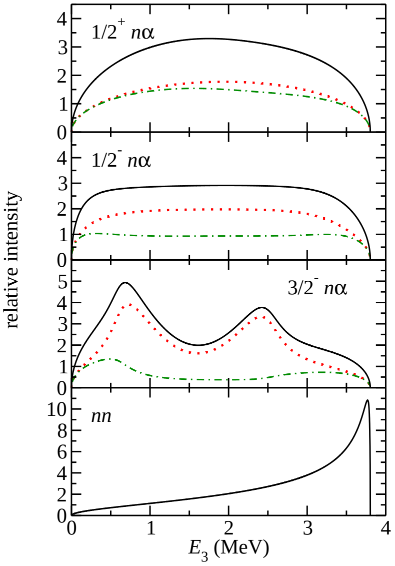

Alpha-particle energy distributions for each channel considered separately. The primary plus secondary, exchange, and total are given by the dotted, dot-dashed, and solid curves, respectively. Only the total is shown for the nn case.

$T(t,2n)\alpha$ Neutron Spectrum Summary / Open Questions

- Only the $3/2^-$ (^{5}He g.s.) provides a distinct feature
- Interpretation of the continuum remains ambiguous
  could this be addressed by a correlation measurement?
- α spectrum?
- $T(t,2n)$ absolute cross section?

Jarmie and Brown, NIM B10/11 405 (1985)
Measured αs – preliminary results...

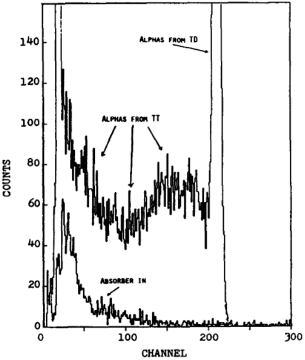

Fig. 8. T(t, α)nn reaction raw data for 45° lab angle and 115 keV bombarding energy. Note the large peak of alpha-particles from the 0.5% deuterium contaminant in the target gas.

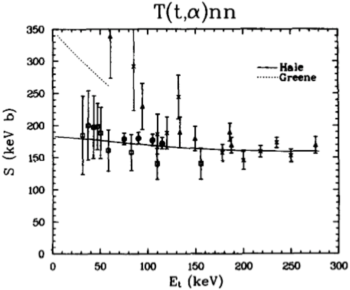

Fig. 9. Integrated *S* functions for the T(t, α)nn reaction. Our preliminary data are the black circles with 5% absolute errors. Also shown are the data of Govorov et al. (triangles) ref. [10]; Agnew et al. (crosses) [11]; and Serov et al. (squares) [12]. The solid curve is an *R*-matrix prediction of Hale [13], and the dashed curve is from the compilation of Greene [14].

Jarmie-Brown Spectrum

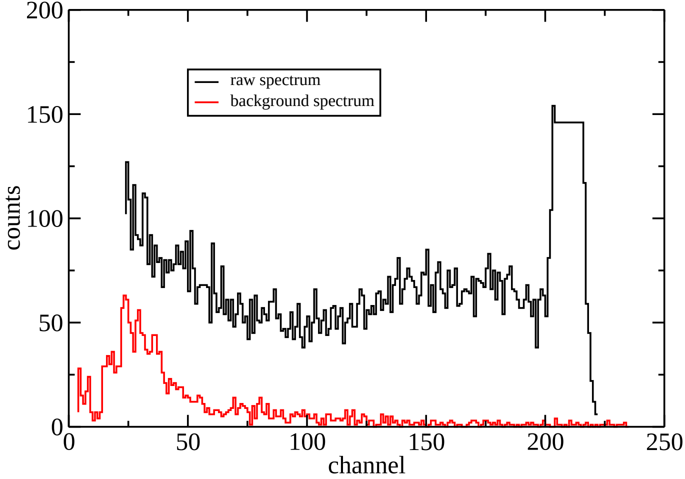

Jarmie-Brown Spectrum Compared to Sayre *et al.* (2013) R-Matrix Fit

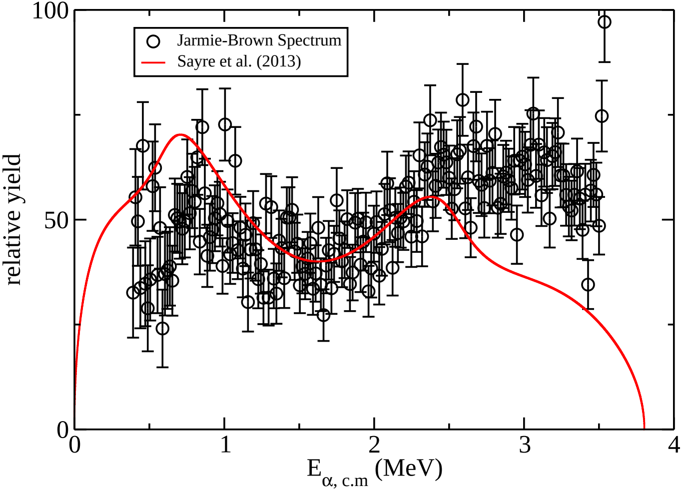

Suggestive of di-neutron strength?

Proton Energy Distributions from $^3He + ^3He$

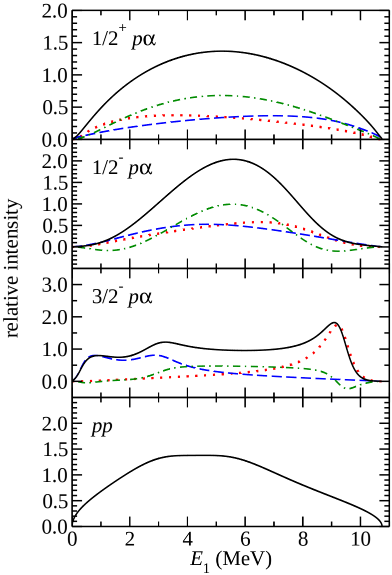

Proton energy distributions from $^3He + ^3He$ for each channel considered separately. The primary, secondary, exchange, and total are given by the dotted, dashed, dot-dashed, and solid curves, respectively. Only the total is shown for the *pp* case.

α Energy Distributions from ^{3}He + ^{3}He

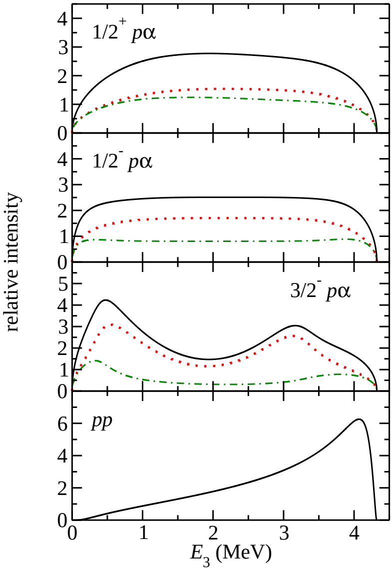

Alpha-particle energy distributions from ^{3}He + ^{3}He for each channel considered separately. The primary, secondary, exchange, and total are given by the dotted, dashed, dot-dashed, and solid curves, respectively. Only the total is shown for the *pp* case.

Coulomb Effects Near the Endpoint

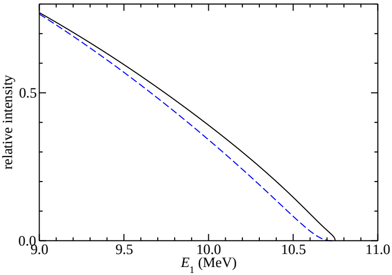

Proton energy distributions from $^3\mathrm{He} + {}^3\mathrm{He}$ for the $1/2^+$ $p\alpha$ channel near the endpoint. The solid curve is the same as shown previously and the dashed curve shows the effect of including an ad-hoc Coulomb correction.

Thank you for your attention.